

# Measurement of chromatic dispersion of microstructured polymer fibers by white-light spectral interferometry

P. Hlubina<sup>a</sup>, D. Ciprian<sup>a</sup>, M. H. Frosz<sup>b</sup>, K. Nielsen<sup>b</sup>

<sup>a</sup>Department of Physics, Technical University Ostrava,  
17. listopadu 15, 708 33 Ostrava-Poruba, Czech Republic

<sup>b</sup>Department of Photonics Engineering, Technical University of Denmark,  
Oersteds Plads 343, DK-2800 Kongens Lyngby, Denmark

## ABSTRACT

We present a white-light spectral interferometric method for measuring the chromatic dispersion of microstructured fibers made of polymethyl methacrylate (PMMA). The method uses an unbalanced Mach-Zehnder interferometer with the fiber of known length placed in one of the interferometer arms and the other arm with adjustable path length. We record the spectral interferograms to measure the equalization wavelength as a function of the path length difference, or equivalently the differential group refractive index dispersion over a wide wavelength range. First, we verify the applicability of the method by measuring the wavelength dependence of the differential group refractive index of a pure silica fiber. We apply a five-term power series fit to the measured data and confirm by its differentiation that the chromatic dispersion of pure silica glass agrees well with theory. Second, we measure the chromatic dispersion for the fundamental mode supported by two different PMMA microstructured fibers, the multimode fiber and the large-mode area one.

**Keywords:** spectral interferometry, Mach-Zehnder interferometer, differential group refractive index, chromatic dispersion, microstructured fiber, PMMA

## 1. INTRODUCTION

Polymer optical fiber (POF) as an expected integral part of datacom networks (the backbone of the critical last mile) offers a high-bandwidth, easy-to-install and fiber-optic replacement for copper cables.<sup>1</sup> In contrast to glass optical fibers, POFs will remain mechanically flexible. The property, in combination with a large core, allows easy and inexpensive connectivity of the POFs during installation. Unfortunately, conventional POF has a number of disadvantages. A persistent problem with POF is the poor performance in relatively humid, high-temperature environments. Traditional large-core multimode step-index POF suffers from very large modal dispersion. The single-mode POF, ideal for telecommunication purposes, is with the associated small mode area that limits the applications. Fortunately, some of the disadvantages of conventional POF are potentially addressed by the use of a new type of POFs, namely microstructured POFs (mPOFs).<sup>2,3</sup>

Hollow-core mPOFs (with a light guiding mechanism which is fundamentally different from that in conventional POFs) and index-guiding mPOFs,<sup>2-5</sup> both offer a range of unique properties and benefits. These include the possibility to combine single-mode behavior with large mode areas and the promise of guidance in air rather than in the fiber material with the effect on the transmission loss that can be reduced by almost 4 orders of magnitude.<sup>4</sup> Some mPOFs allow for localized biosensing,<sup>6</sup> optical sensing<sup>7</sup> and an elaborate dispersion control.<sup>8</sup>

The huge interest in silica photonic crystal fiber (PCFs) has largely been due to the possibility of manipulating the dispersion profile by modifying the microstructure. This has allowed researchers to shift the zero-dispersion wavelength of silica fibers to below 800 nm by reducing the core size. The combination of a small core size and zero-dispersion wavelength at the operating wavelength of widely available femtosecond Ti:sapphire lasers led to an extensive research in supercontinuum generation and other nonlinear effects in PCFs.<sup>9</sup> It is crucial

---

Further author information:

P. Hlubina: E-mail: petr.hlubina@vsb.cz, phone: +420 (59) 732-3134, fax: +420 (59) 732-3403

M. H. Frosz: E-mail: mhfr@fotonik.dtu.dk, phone: +45 4525-6369

for the efficiency of many nonlinear mechanisms that the pump laser wavelength is close to the zero-dispersion wavelength and that the core size is small. Recently, work in fabricating PCFs from materials other than silica, such as polymer materials, has intensified. One of the advantages is that the fabrication of polymer fibers requires a factor of ten lower temperature, and therefore much simpler equipment and processing. As with silica PCFs, it is difficult to accurately obtain a small core size while maintaining small structural variations during fiber drawing. This has limited the possibilities of dispersion engineering in mPOFs.

The chromatic dispersion, which can be obtained by simply differentiating the measured relative group refractive index, belongs to one of the fundamental dispersion characteristics of optical fibers. Chromatic dispersion of long length optical fibers is determined by two widely used methods: the time-of-flight method<sup>10,11</sup> and the modulation phase shift technique.<sup>11</sup> White-light interferometry based on the use of a broadband source in combination with a standard Michelson or Mach-Zehnder interferometer<sup>12</sup> is considered as one of the best tools for dispersion characterization of short length optical fibers. White-light interferometry usually utilizes a temporal method<sup>13,14</sup> or a spectral method.<sup>15-20</sup> The dispersion characteristics of the fibers under study can also be obtained by other interferometric techniques.<sup>21-24</sup>

The spectral method is based on the observation of spectral interference fringes in the vicinity<sup>15-19</sup> of a stationary phase point or far from it<sup>20</sup> and involves measurement of the phase or period of the spectral fringes. The stationary phase point appears in the recorded spectrum when the overall group optical path difference (OPD) between two beams in the interferometer is close to zero. Recently, the use of the method with a Mach-Zehnder interferometer was extended for dispersion characterization of tapered fibers<sup>19</sup> or glasses of optical fibers.<sup>25</sup> The feasibility of the interferometric techniques has been demonstrated in measuring the dispersion in air-silica microstructured optical fibers.<sup>26-30</sup>

In this paper, a technique based on white-light interferometry<sup>25,30</sup> is used for measuring the chromatic dispersion of mPOFs made of PMMA. The technique comprises the recording of a series of the spectral interferograms in a Mach-Zehnder interferometer with the fiber of known length placed in one of the interferometer arms and the other arm with adjustable path length. We measured the equalization wavelength as a function of the path length difference, or equivalently the differential group refractive index dispersion over a wide wavelength range. First, we verify the applicability of the method by measuring the wavelength dependence of the differential group refractive index of a pure silica fiber. We apply a five-term power series fit to the measured data and confirm by its differentiation that the chromatic dispersion of pure silica glass agrees well with theory. Second, we measure the chromatic dispersion for the fundamental mode supported by two different PMMA microstructured fibers, the multimode mPOF and the large-mode area one.

## 2. EXPERIMENTAL METHOD

### 2.1. Differential group refractive index measurement

Consider an unbalanced Mach-Zehnder interferometer as shown in Fig. 1 with a fiber under test of length  $z$  and of the phase refractive index  $n(\lambda)$ .<sup>25,30,31</sup> The fiber is placed in the first (test) arm of the interferometer that comprises optical components such as lens 1 and lens 2 to which the effective thickness  $d$  and the phase refractive index  $n_c(\lambda)$  correspond. The other (reference) arm is with the adjustable path length  $L$  in the air so that the group OPD  $\Delta_{\text{MZ}}^g(\lambda)$  between the beams in the interferometer is given by

$$\Delta_{\text{MZ}}^g(\lambda) = L - l - N(\lambda)z - N_c(\lambda)d, \quad (1)$$

where  $l$  is the path length in the air in the test arm and  $N(\lambda)$ ,  $N_c(\lambda)$  are the group refractive indices.

Consider now that the spectral interferogram recorded in the setup have the largest period in the vicinity of a stationary phase point for which the group OPD is zero at one specific wavelength  $\lambda_0$ , referred to as the equalization wavelength.<sup>30</sup> The condition  $\Delta_{\text{MZ}}^g(\lambda_0) = 0$  gives for the overall path length  $L = L_o = L_o(\lambda_0)$  for which the equalization wavelength  $\lambda_0$  is resolved in the recorded spectrum the relation

$$L_o(\lambda_0) = N(\lambda_0)z + N_c(\lambda_0)d + l. \quad (2)$$

If we choose one of the equalization wavelengths,  $\lambda_{0r}$ , as the reference one, we can introduce the overall path length difference  $\Delta L_o(\lambda_0) = L_o(\lambda_0) - L_o(\lambda_{0r})$  given by

$$\Delta L_o(\lambda_0) = \Delta N(\lambda_0)z + \Delta N_c(\lambda_0)d, \quad (3)$$

where  $\Delta N(\lambda_0) = N(\lambda_0) - N(\lambda_{0r})$  and  $\Delta N_c(\lambda_0) = N_c(\lambda_0) - N_c(\lambda_{0r})$  are the corresponding differential group refractive indices.

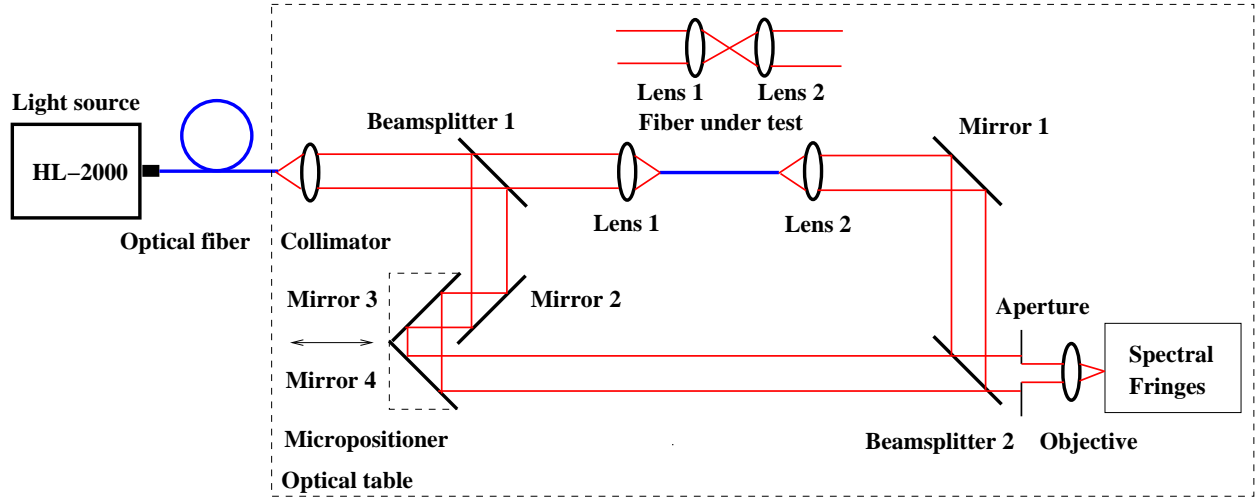


**Figure 1.** Experimental setup with an unbalanced Mach-Zehnder interferometer to measure the group refractive index dispersion of a fiber under test.

Next, consider the unbalanced Mach-Zehnder interferometer in which the fiber is removed and which is used for measuring the group dispersion of the optical components. This group dispersion has to be subtracted from the overall group dispersion to determine the group dispersion of the fiber alone. The group OPD  $\Delta_{\text{MZ}}^g(\lambda)$  between the beams in the interferometer is after the removal of the fiber given by

$$\Delta_{\text{MZ}}^g(\lambda) = L - l - z - N_c(\lambda)d. \quad (4)$$

The condition  $\Delta_{\text{MZ}}^g(\lambda_0) = 0$  gives for the corresponding path length  $L = L_c = L_c(\lambda_0)$  for which the equalization wavelength  $\lambda_0$  is resolved in the recorded spectrum the relation

$$L_c(\lambda_0) = N_c(\lambda_0)d + l + z. \quad (5)$$

If we choose the same reference equalization wavelength  $\lambda_{0r}$  as in the previous step (with the fiber), the corresponding path length difference denoted as  $\Delta L_c(\lambda_0) = L_c(\lambda_0) - L_c(\lambda_{0r})$  is given by

$$\Delta L_c(\lambda_0) = \Delta N_c(\lambda_0)d. \quad (6)$$

Using Eqs. (3) and (6), we obtain the relation

$$\Delta N(\lambda_0) = [\Delta L_o(\lambda_0) - \Delta L_c(\lambda_0)]/z, \quad (7)$$

which means that the differential group refractive index  $\Delta N(\lambda_0)$  of the fiber, namely that of the core mode supported by the fiber,<sup>30</sup> can be measured directly as a function of the equalization wavelength  $\lambda_0$ .

The measured wavelength dependence of the differential group refractive index can be fitted to a function  $\Delta N(\lambda)$  from which the chromatic dispersion  $D(\lambda)$  also known as the group velocity dispersion (GVD) can be evaluated by using the relation

$$D(\lambda) = \frac{d}{d\lambda} \frac{1}{v_g(\lambda)} = \frac{1}{c} \frac{dN(\lambda)}{d\lambda} = \frac{1}{c} \frac{d\Delta N(\lambda)}{d\lambda}, \quad (8)$$

where  $v_g(\lambda)$  is the group velocity and  $c$  is the velocity of light in vacuum.

## 2.2. Material dispersion

### 2.2.1. Pure silica glass

The wavelength-dependent refractive index of pure silica glass can be approximated by the semi-empirical Sellmeier dispersion equation<sup>33,34</sup>

$$n^2(\lambda) = 1 + \sum_{i=1}^3 \frac{A_i \lambda^2}{(\lambda^2 - B_i^2)}, \quad (9)$$

where the coefficients are for the temperature of 20 °C and the wavelength in the micrometers as follows:<sup>33,34</sup>  $A_1 = 0.6961663$ ,  $A_2 = 0.4079426$ ,  $A_3 = 0.8974794$ ,  $B_1 = 0.0684043$ ,  $B_2 = 0.1162414$  and  $B_3 = 9.896161$ . The corresponding group refractive index  $N(\lambda)$  is given by

$$N(\lambda) = n(\lambda) - \lambda \frac{dn(\lambda)}{d\lambda} = n(\lambda) + \frac{\lambda^2}{n(\lambda)} \sum_{i=1}^3 \frac{A_i B_i^2}{(\lambda^2 - B_i^2)^2}, \quad (10)$$

where the refractive index  $n(\lambda)$  is given by Eq. (9). Equation (10) gives

$$\frac{dN(\lambda)}{d\lambda} = \frac{N(\lambda)}{\lambda n(\lambda)} [N(\lambda) - n(\lambda)] - \frac{4\lambda^3}{n(\lambda)} \sum_{i=1}^3 \frac{A_i B_i^2}{(\lambda^2 - B_i^2)^3}, \quad (11)$$

which is needed in the evaluation of the material dispersion  $D(\lambda) = D_m(\lambda)$  of the pure silica glass according to Eq. (8).

### 2.2.2. Bulk PMMA

The wavelength-dependent refractive index of bulk PMMA can be approximated by the dispersion equation<sup>35</sup>

$$n^2(\lambda) = A_0 + A_1 \lambda^2 + A_2 \lambda^{-2} + A_3 \lambda^{-4} + A_4 \lambda^{-6} + A_5 \lambda^{-8}, \quad (12)$$

where the coefficients are for the wavelength in the micrometers as follows:<sup>35</sup>  $A_0 = 2.18645820$ ,  $A_1 = -2.4475348 \times 10^{-4}$ ,  $A_2 = 1.4155787 \times 10^{-2}$ ,  $A_3 = -4.4329781 \times 10^{-4}$ ,  $A_4 = 7.7664259 \times 10^{-5}$  and  $A_5 = -2.9936382 \times 10^{-6}$ . The material dispersion  $D_m(\lambda)$  of the bulk PMMA can be evaluated in a similar way as that of the pure silica glass.

## 3. EXPERIMENTAL SETUP

The setup used for measuring the differential group refractive index dispersion or the chromatic dispersion of the core modes supported by mPOFs is shown in Fig. 1. It consists of a white-light source: a quartz-tungsten-halogen lamp (HL-2000HP, Ocean Optics) with launching optics, a single-mode optical fiber (FS-SN-3224, 3M), a collimating lens, a bulk-optic Mach-Zehnder interferometer with plate beamsplitters (BSW07, Thorlabs), a micropositioner connected to mirrors 3 and 4 of the interferometer, an aperture, a Glan-Taylor polarizer (Thorlabs), a microscope objective, micropositioners, a fiber-optic spectrometer (S2000, Ocean Optics), an A/D converter and a personal computer. In the test arm of the interferometer is placed a combination of a fiber sample and optical components (shown schematically in Fig. 1 as lens 1 and lens 2) represented by a microscope objective (10×/0.30, Meopta), and an achromatic lens (74-ACR, Ocean Optics, Inc.). The spectrometers S2000 has a spectral operation range from 350 to 1000 nm. The fiber sample is in the case of the reference measurement pure silica holey fiber (PM-1550-01, Thorlabs)<sup>26</sup> of length  $z = (50650 \pm 10) \mu\text{m}$ .

The chromatic dispersion was measured for two different mPOFs, multimode fiber and large-mode area one. We have fabricated mPOFs in the polymer PMMA with core sizes down to about 2-3  $\mu\text{m}$  diameter using a simple two-step process. The PMMA fiber preform with holes (2 mm diameter) is first drawn into a cane, reducing the structure by a factor of  $\approx 10$ . The cane is then inserted into a PMMA tube and drawn into a fiber, reducing the structure by an additional factor of  $\approx 200$ . The multimode mPOF has diameter of 142  $\mu\text{m}$ , pitch of 4  $\mu\text{m}$ , hole size of 3  $\mu\text{m}$  and length  $z = (54300 \pm 10) \mu\text{m}$ . The large-mode area mPOF, approximately 250  $\mu\text{m}$  in diameter, has 11  $\mu\text{m}$  pitch, 4  $\mu\text{m}$  hole size and length  $z = (58560 \pm 10) \mu\text{m}$ .

## 4. EXPERIMENTAL RESULTS AND DISCUSSION

Prior to the chromatic dispersion measurements of mPOFs we verified the functionality of our method in measuring the chromatic dispersion of pure silica glass. We used a laser diode instead of the halogen lamp to check the precise placement and alignment of the optical components in the test arm by observing the interference fringes. Then we used air-silica microstructured fiber<sup>25</sup> and the excitation of the outer fiber cladding (made of pure silica), which was easily inspected at the output of the test arm when the ring-shape optical field was observed.

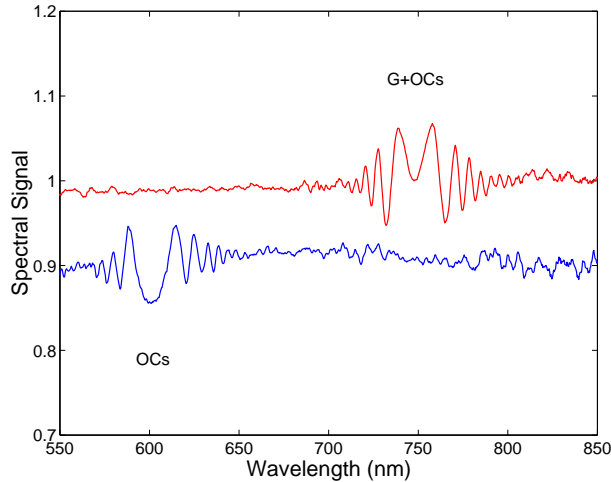


**Figure 2.** Examples of the spectral signals recorded for two cases: optical components (OCs), outer fiber cladding (pure silica glass) plus optical components (F+OCs).

First, the dispersion measurement was performed for the optical components for which the equalization wavelength cannot be resolved with the unbalanced Mach-Zehnder interferometer alone. A method of tandem interferometry<sup>32</sup> was used, which utilizes a Michelson interferometer placed between the source and the unbalanced Mach-Zehnder interferometer and an appropriate path length difference in the Michelson interferometer was adjusted to resolve the spectral interference fringes at the output of the Mach-Zehnder interferometer.<sup>25</sup> Figure 2 shows an example of the recorded spectral signal (denoted as OCs) obtained by subtracting the reference signal (without the interference) from the interferogram. It clearly shows that the spectral interference fringes can be identified only in the vicinity of the equalization wavelength  $\lambda_0 = 601.35$  nm. Next, the dispersion measurements of the outer cladding were performed on a combination of the fiber and optical components in the setup shown in Fig. 1. In the measurements, such a path length in the reference arm of the interferometer was adjusted to resolve spectral interference fringes. Figure 2 shows an example of the recorded spectral signal corresponding to the excitation of the outer fiber cladding (denoted as G+OCs). It clearly shows the spectral interference fringes identified only in the vicinity of the equalization wavelength  $\lambda_0 = 748.23$  nm.

During the dispersion measurement of the pure silica glass we adjusted such a path length in the reference arm of the interferometer that allows to resolve spectral interference fringes. To reveal the dependence of the equalization wavelength on the adjusted path length, we displaced manually the stage with mirrors 3 and 4 by using the micropositioner with a constant step of  $10 \mu\text{m}$  and recorded the corresponding spectral signals. The spectral signals recorded for the optical components revealed that the equalization wavelength  $\lambda_0$  can be resolved in the spectral range from 509 to 869 nm and that the path length difference  $\Delta L_c(\lambda_0)$  varies from 470 to  $-90 \mu\text{m}$ , when the equalization wavelength  $\lambda_{0r} = 748.23$  nm was chosen as the reference one. The measured values are shown in Fig. 3 by the crosses (denoted as OCs) together with the polynomial fit. The spectral signals recorded for the pure silica glass (excitation of the outer fiber cladding) revealed that the equalization wavelength  $\lambda_0$  can be resolved in the spectral range from 508 to 910 nm and that the path length difference  $\Delta L_o$  varies from 1480

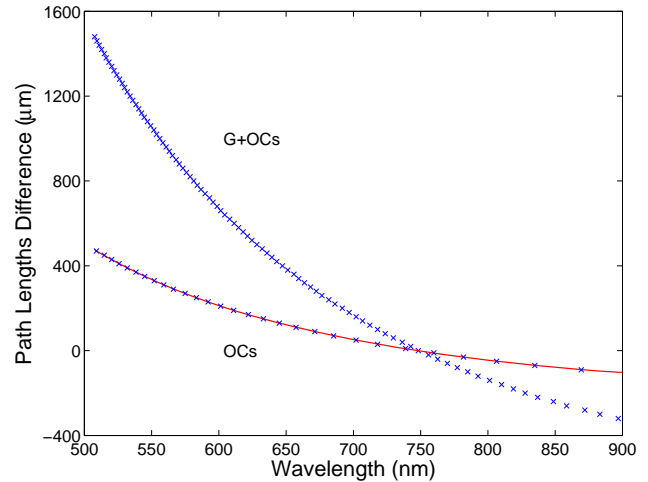


**Figure 3.** Path length difference measured as a function of wavelength for two cases: optical components (OCs), outer fiber cladding (pure silica glass) plus optical components (G+OCs). Solid line is a polynomial fit.

to  $-340 \mu\text{m}$ , when the same reference equalization wavelength was chosen. The measured values are shown in Fig. 3 by the crosses (denoted as G+OCs). Knowledge of the measured dependences and the fiber length  $z$  enables us to evaluate directly the differential group refractive index  $\Delta N(\lambda_0)$  of the pure silica as a function of the equalization wavelength  $\lambda_0$ . The function is represented in Fig. 4 by the crosses and it is shown together with a fit using a five-term power series<sup>36</sup>  $\Delta N(\lambda) = a_1\lambda^4 + a_2\lambda^2 + a_3 + a_4\lambda^{-2} + a_5\lambda^{-4}$ . The chromatic dispersion  $D_m(\lambda)$  corresponding to the above fit is shown in Fig. 5 together with the material dispersion of pure silica glass evaluated by using Eqs. (8) and (11). Figure 5 demonstrates very good agreement between experiment and theory, which supports an applicability of the above method for measuring the chromatic dispersion of other fibers such as mPOFs.

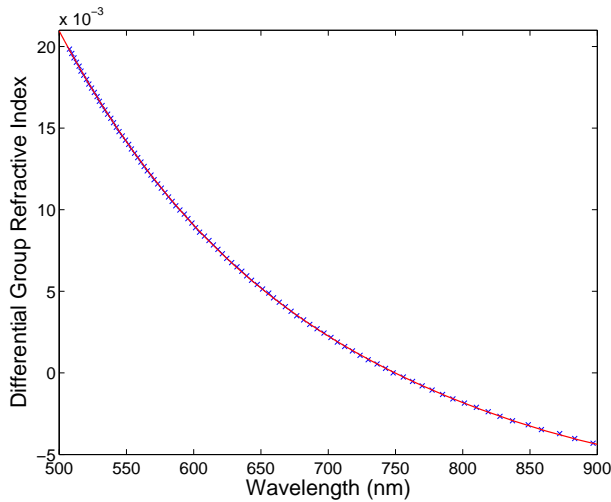


**Figure 4.** Differential group index of outer fiber cladding (pure silica glass) measured as a function of wavelength. The solid line is a five-term power series fit.

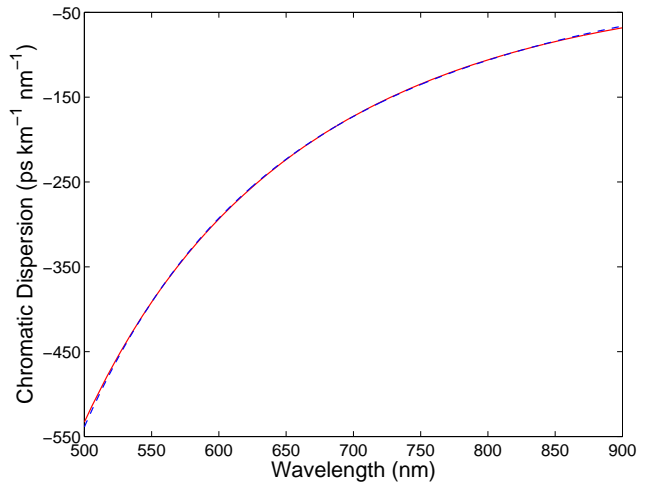


**Figure 5.** Measured chromatic dispersion of the pure silica glass. The dashed line corresponds to the material dispersion of pure silica glass.

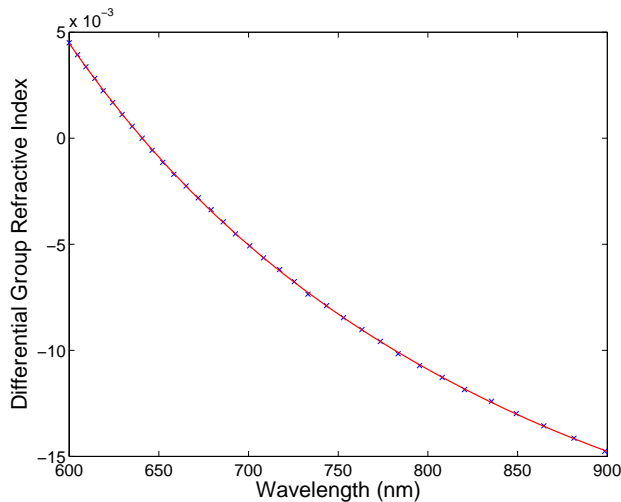


**Figure 6.** Differential group index of the fundamental mode supported by a multimode mPOF measured as a function of wavelength. The solid line is a five-term power series fit.

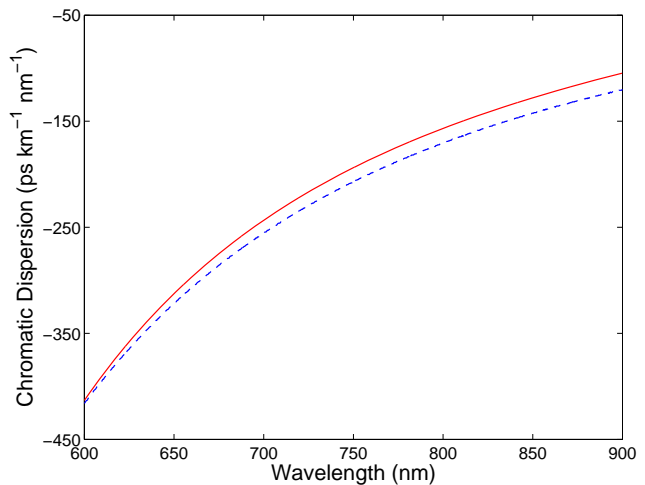


**Figure 7.** Measured chromatic dispersion of the fundamental mode supported by a multimode mPOF. The dashed line corresponds to the material dispersion of a bulk PMMA.

Next, the differential group refractive index dispersion was measured for the fundamental mode supported by a multimode mPOF. Figure 6 shows the measured values by the crosses together with a five-term power series

fit. The chromatic dispersion  $D(\lambda)$  evaluated from the fit by using Eq. (8) is shown in Fig. 7. In the same figure is shown the material dispersion  $D_m(\lambda)$  of bulk PMMA evaluated by using Eqs. (8) and (12). It is clearly seen that the chromatic dispersion for the fundamental mode of the multimode mPOF is higher than that for the bulk PMMA so that the mPOF acts nearly as dispersion shifted fiber. The difference between  $D(\lambda)$  and  $D_m(\lambda)$  that can be attributed to the waveguide dispersion  $D_w(\lambda)$  is higher for longer wavelengths than for shorter ones. This behaviour is expected due to the well-known fact that the contribution from waveguide dispersion increases with wavelength (see, e.g., Fig. 1 in Ref. [37]). Physically, this is because the mode is well-confined to the core for short wavelengths, and the light therefore primarily interacts with the bulk material; as the mode size increases with wavelength, the light will increase its interaction with the surrounding air-holes.

Finally, the differential group refractive index dispersion was measured for the fundamental mode supported by a large-mode area (LMA) mPOF. Figure 8 shows the measured values by the crosses together with a five-term power series fit. The chromatic dispersion  $D(\lambda)$  evaluated from the fit by using Eq. (8) is shown in Fig. 9. In the same figure is shown the material dispersion  $D_m(\lambda)$  of bulk PMMA. It is clearly seen that the chromatic dispersion for the fundamental mode of the LMA mPOF is similar to that for the bulk PMMA. There is no significant effect of the waveguide dispersion  $D_w(\lambda) = D(\lambda) - D_m(\lambda)$ . This is also expected physically, since in the LMA fiber the fraction of the mode area overlapping with the air-holes is smaller than in the multimode fiber.

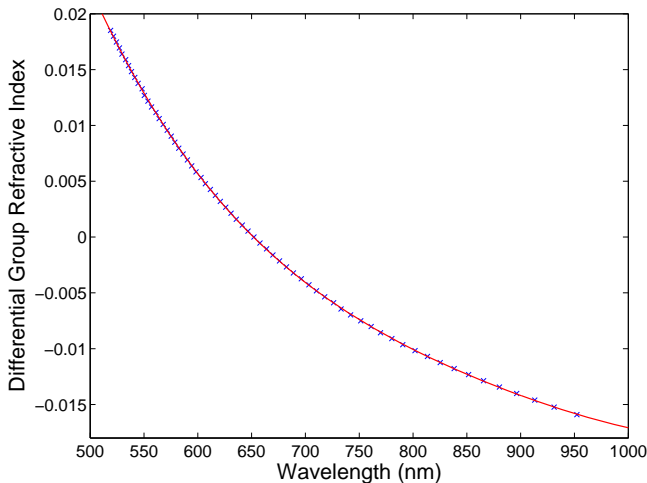


**Figure 8.** Differential group index of the fundamental mode supported by an LMA mPOF measured as a function of wavelength. The solid line is a five-term power series fit.

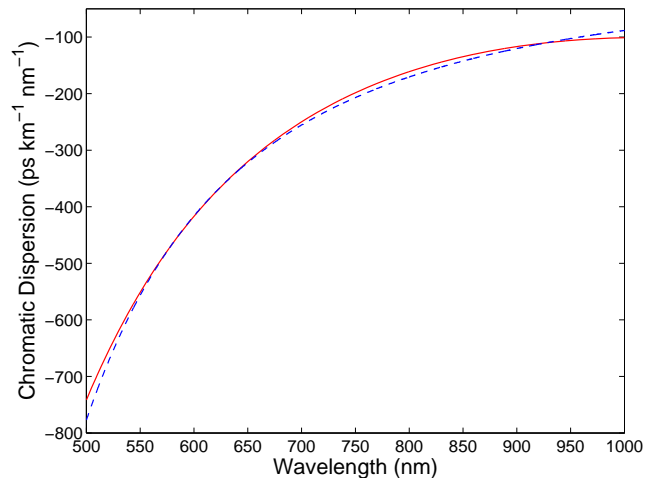


**Figure 9.** Measured chromatic dispersion of the fundamental mode supported by an LMA mPOF. The dashed line corresponds to the material dispersion of a bulk PMMA.

## 5. CONCLUSIONS

We presented the results of chromatic dispersion measurement of two mPOFs obtained by using a white-light spectral interferometric method. The technique utilizes the recording of a series of the spectral interferograms in a Mach-Zehnder interferometer with the fiber of known length placed in one of the interferometer arms and the other arm with adjustable path length. The equalization wavelength as a function of the path length difference, or equivalently the group refractive index dispersion was measured. First, we verified the applicability of the method by measuring the wavelength dependence of the differential group refractive index of a pure silica fiber. We applied a five-term power series fit to the measured data and confirmed by its differentiation that the chromatic dispersion of pure silica glass agrees well with theory. Second, we measured the chromatic dispersion for the fundamental mode supported by two different mPOFs made of PMMA, the multimode mPOF and the large-mode area one. The results obtained demonstrate that the mPOFs allow for an elaborate dispersion control.

## ACKNOWLEDGMENTS

The research was partially supported by grant MSM6198910016 and by the COST Action 299 (project No. OC09020).

## REFERENCES

1. J. Zubia and J. Arrue, "Plastic optical fibers: An introduction to their technological processes and applications," *Opt. Fiber Technol.* **7**, pp. 101–140, 2001.
2. M. A. van Eijkelenborg, M. C. J. Large, A. Argyros, J. Zagari, S. Manos, N. Issa, I. Bassett, S. Fleming, R. C. Mc Phedran, C. M. de Sterke, N. A. P. Nicorovici, "Microstructured polymer optical fibre," *Opt. Express* **9**, pp. 319–327, 2001.
3. M. A. van Eijkelenborg, A. Argyros, G. Barton, I. M. Bassett, M. Fellow, G. Henry, N. A. Issa, M. C. J. Large, S. Manos, W. Padden, L. Poladian, J. Zagari, "Recent progress in microstructured polymer optical fibre fabrication and characterisation," *Opt. Fiber Technol.* **9**, pp. 199–209, 2003.
4. A. Argyros and J. Pla, "Hollow-core polymer fibres with a kagome lattice: potential for transmission in the infrared," *Opt. Express* **16**, pp. 16896–16908, 2007.
5. M. A. van Eijkelenborg, A. Argyros, and S. G. Leon-Saval, "Polycarbonate hollow-core microstructured optical fiber," *Opt. Lett.* **33**, pp. 2446–2448, 2008.
6. G. Emiliyanov, J. B. Jensen, O. Bang, P. E. Hoiby, L. H. Pedersen, E. M. Kjær, and L. Lindvold, "Localized biosensing with Topas microstructured polymer optical fiber," *Opt. Lett.* **32**, pp. 460–462, 2007.
7. X. Yang and L. Wang, "Silver nanocrystals modified microstructured polymer optical fibres for chemical and optical sensing," *Opt. Commun.* **280**, pp. 368–373, 2007.
8. M. Bache, "Designing microstructured polymer optical fibers for cascaded quadratic soliton compression of femtosecond pulses," *J. Opt. Soc. Am. B* **26**, pp. 460–470, 2009.
9. J. M. Dudley, G. Genty, and S. Coen, "Supercontinuum generation in photonic crystal fiber," *Rev. Mod. Phys.* **78**, pp. 1135–1185, 2006.
10. J. H. Wiesenfeld and J. Stone, "Measurement of dispersion using short lengths of an optical fiber and picosecond pulses from semiconductor film lasers," *J. Lightwave Technol.* **2**, pp. 464–468, 1984.
11. L. G. Cohen, "Comparison of single-mode fiber dispersion measurement techniques," *J. Lightwave Technol.* **3**, pp. 958–966, 1985.
12. S. Diddams and J. C. Diels, "Dispersion measurements with white-light interferometry," *J. Opt. Soc. Am. B* **13**, pp. 1120–1128, 1995.
13. M. Tateda, N. Shibata, and S. Seikai, "Interferometric method for chromatic dispersion measurement in a single-mode optical fiber," *IEEE J. Quantum Electron.* **17**, pp. 404–407, 1981.
14. M. J. Saunders and W. B. Gardner, "Interferometric determination of dispersion variations in single-mode fibers," *J. Lightwave Technol.* **5**, pp. 1701–1705, 1987.
15. J. Pelayo, J. Paniello, and F. Villuendas, "Chromatic dispersion characterization in short single-mode fibers by spectral scanning of phase difference in a Michelson interferometer," *J. Lightwave Technol.* **6**, pp. 1861–1865, 1988.
16. P. Merritt, R. P. Tatam, and D. A. Jackson, "Interferometric chromatic dispersion measurements on short lengths of monomode optical fiber," *J. Lightwave Technol.* **7**, pp. 703–716, 1989.
17. F. Koch, S. V. Chernikov, and J. R. Taylor, "Dispersion measurement in optical fibres over the entire spectral range from 1.1  $\mu\text{m}$  to 1.7  $\mu\text{m}$ ," *Opt. Commun.* **175**, pp. 209–213, 2001.
18. Y. C. Zhao and S. Fleming, "Direct measurement for second-order dispersion using multi-section interference fringes in spectral domain," *Meas. Sci. Technol.* **16**, pp. 1628–1630, 2005.
19. P. Lu, H. Ding, and S. J. Mihailov, "Direct measurement of the zero-dispersion wavelength of tapered fibres using broadband-light interferometry," *Meas. Sci. Technol.* **16**, pp. 1631–1636, 2005.
20. J. Y. Lee and D. Y. Kim, "Versatile chromatic dispersion measurement of a single mode fiber using spectral white light interferometry," *Opt. Express* **14**, pp. 11608–11614, 2006.
21. J. Brendel, H. Zbinden, and N. Gisin, "Measurement of chromatic dispersion in optical fibers using pairs of correlated photons," *Opt. Commun.* **151**, pp. 35–39, 1998.

22. K. S. Abedin, M. Hyodo, and N. Onodera, "Measurement of the chromatic dispersion of an optical fiber by use of a Sagnac interferometer employing asymmetric modulation," *Opt. Lett.* **25**, pp. 299–301, 2000.
23. H. Chi and J. Yao, "Fiber chromatic dispersion measurement based on wavelength-to-time mapping using a femtosecond pulse laser and an optical comb filter," *Opt. Commun.* **280**, pp. 337–342, 2007.
24. M. A. Galle, W. Mohammed, L. Qian, and P. W. E. Smith, "Single-arm three-wave interferometer for measuring dispersion of short lengths of fiber," *Opt. Express* **16**, pp. 16896–16908, 2007.
25. P. Hlubina, R. Chlebus, and D. Ciprian, "Differential group refractive index dispersion of glasses of optical fibres measured by a white-light spectral interferometric technique," *Meas. Sci. Technol.* **18**, pp. 1547–1552, 2007.
26. P. Hlubina, M. Szpulak, L. Knyblová, G. Statkiewicz, T. Martynkien, D. Ciprian, and W. Urbańczyk, "Measurement and modelling of dispersion characteristics of two-mode birefringent holey fibre," *Meas. Sci. Technol.* **17**, pp. 626–630, 2006.
27. D. Ouzounov, D. Homoelle, W. Zipfel, W. W. Webb, A. L. Gaeta, J. A. West, J. C. Fajardo, and K. W. Koch, "Dispersion measurements of microstructure fibers using femtosecond laser pulses," *Opt. Commun.* **192**, pp. 219–223, 2001.
28. Q. Ye, C. Xu, X. Liu, W. H. Knox, M. F. Yan, R. S. Windeler, and B. Eggleton, "Dispersion measurement of tapered airsilica microstructure fiber by white-light interferometry," *Appl. Opt.* **41**, pp. 4467–4470, 2002.
29. L. Labonté, P. Roy, F. Pagnoux, F. Louradour, C. Restoin, G. Mélin, and E. Burov, "Experimental and numerical analysis of the chromatic dispersion dependence upon the actual profile of small core microstructured fibres," *J. Opt. A: Pure App. Opt.* **8**, pp. 933–938, 2006.
30. P. Hlubina, M. Szpulak, D. Ciprian, T. Martynkien, and W. Urbańczyk, "Measurement of the group dispersion of the fundamental mode of holey fiber by white-light spectral interferometry," *Opt. Express* **15**, pp. 11073–11081, 2007.
31. P. Hlubina, D. Ciprian, R. Chlebus, "Group index dispersion of holey fibres measured by a white-light spectral interferometric technique," *Opt. Commun.* **281**, pp. 4008–4013, 2008.
32. R. Chlebus, P. Hlubina, and D. Ciprian, "Spectral-domain tandem interferometry to measure the group dispersion of optical samples," *Opt. Lasers Eng.* **47**, pp. 173–179, 2009.
33. I.H. Malitson, "Interspecimen comparison of the refractive index of fused silica," *J. Opt. Soc. Am.* **55**, pp. 1205–1209, 1965.
34. P. Hlubina, "White-light spectral interferometry with the uncompensated Michelson interferometer and the group refractive index dispersion in fused silica," *Opt. Commun.* **193**, pp. 1–7, 2001.
35. Dispersion data provided by Optical Fibre Technology Centre, University of Sydney, Australia.
36. P. Peterka, J. Kaňka, P. Honzátko, and D. Káčik, "Measurement of chromatic dispersion of microstructure optical fibers using interferometric method," *Opt. Appl.* **38**, pp. 295–303, 2008.
37. M. H. Frosz, P. M. Moselund, P. D. Rasmussen, C. L. Thomsen, and O. Bang, "Increasing the blue-shift of a supercontinuum by modifying the fiber glass composition," *Opt. Express* **16**, pp. 21076–21086, 2008.